Journal of Physics: Conference Series **192** (2009) 012001 doi:10.1088/1742-6596/192/1/012001

Excited core states in the dissociative recombination of N_2^+

Steven L Guberman

Institute for Scientific Research, 22 Bonad Road, Winchester, MA 01890, USA

slg@sci.org

Abstract. Theoretical studies of dissociative recombination along the $b'^1\Sigma_u^+$ dissociative route of N_2 from the v=0 level of the $X^2\Sigma_g^+$ ion are described. Rydberg states having both the ground $X^2\Sigma_g^+$ and $A^2\Pi_u$ cores are included in the calculation of cross sections and rate constants. The electronic width connecting these Rydberg series is zero. Nevertheless, the two Rydberg series are connected through the dissociative state. The large electronic width for the $A^2\Pi_u$ Rydberg states leads to a factor of 20 decrease in the rate constant at 1000 K electron temperature.

1. Introduction

Dissociative recombination (DR) is driven by variants of the direct [1] and indirect [2] mechanisms. The interference between these two mechanisms determines the shapes of cross sections and rate coefficients. For many years, the indirect DR mechanism was described using only Rydberg states having an ionic core that is identical to the state of the recombining ion. However, the energetics are often such that Rydberg states with an excited ion core are also accessible by low energy electrons undergoing capture by the ground ion state. The vibrational levels of both the ground and excited core Rydberg (ECR) states which lie above the lowest vibrational level of the ground core are resonances and they are the source of considerable structure in DR cross sections.

DR through ECR states has been discussed previously for N_2^+ [3-5], CD^+ [6-9], CH^+ [7-9], OH^+ [10] and H_2^+ [11]. For H_2^+, ECR states dominate DR since all the dissociative states are of this character. In this paper, I examine the role of excited core states in the DR of N_2^+ by focusing upon DR within $^1\Sigma_u^+$ symmetry. Prior theoretical studies have shown that the $^3\Pi_u$ states of N_2^+ are the dominant routes for DR [3-5, 12]. The additional dissociative routes for the lowest 5 ion vibrational levels are states of $^1\Pi_u$, $^1\Sigma_g^+$, $^1\Sigma_u^+$, $^3\Pi_g$, $^3\Sigma_u^+$ and $^3\Sigma_g^+$ symmetries. Prior studies have shown that for $^3\Pi_u$, the addition of ECR $^3\Pi_u$ states leads to a 10% increase in the total room temperature DR rate constant [4] from v=0. For $2^1\Sigma_g^+$, the ECR states increase the room temperature DR rate constant along $2^1\Sigma_g^+$ from v=0 by a factor of 4 but because the rate constant is small [5], there is only a small change in the total rate constant due to all routes.

In the next section, the potential curve calculations for $^1\Sigma_u^+$ are described. A description of the calculation of the widths and quantum defects is in section 3. The cross sections are analyzed in section 4 and the conclusions follow in section 5.

2. Potential curves

The potential curve for the $b'^1\Sigma_u^+$ state has been calculated using the same approach described previously [5] for the $2^1\Sigma_g^+$ route with one exception. With the cc-pVQZ basis of Dunning [13], Rydberg character mixes into the wave function at energies just above the ion potential curve. However, in the model used here, all states are diabatic, i.e. they have purely valence or Rydberg character. If the dissociative state were fully optimized, i.e. if we allowed Rydberg character to mix in, the dissociative state would not cross the ion and a different model of DR would be required. The widths described in the next section are between diabatic valence and Rydberg states. In order for the widths to be appropriate for the valence dissociative state, any Rydberg character must be projected out. The projection is done in an approximate manner by removing the most diffuse contracted basis function in each of the s and p Gaussians. Each of these basis functions is a single primitive. The resulting contracted basis consisted of 4s, 3p, 3d, 2f, 1g contracted functions. The ion curve used previously [5] was shifted in energy by placing it at the experimental ionization energy [14] above the ground state of N_2, also calculated in the above basis. The curves are shown in figure 1. The dissociative curve crosses the ion ground state at the small R turning point of the v=0 level of the ion ground state. The large R asymptote of the b′ state lies at an experimental energy of 0.137 eV [14, 15] above the v=0 ion level. DR does not take place along this route until the electron energy exceeds 0.137 eV and the DR rate constant is small for room temperature electrons. Also shown in figure 1a is the $3\pi_g\ ^1\Sigma_u^+$ Rydberg state of the $A^2\Pi_u$ core. The first accessible vibrational level for DR is v=2 since the lowest two vibrational levels lie below the v=0 ion level. For the neighboring state with the $4\pi_g$ orbital (figure 1b), the lowest accessible vibrational level is v=0. We will return to these potential curves in the discussion of the cross sections in section 4.

3. Widths and Quantum Defects

The width for electron capture into the dissociative state is given by

$$\Gamma^{\varepsilon}_{ion,d}(R)=2\pi <\{\Phi_{ion}(x, R)\ \varphi_{\varepsilon}(x, R)\}\ |H\ |\ \Phi_d(x, R)>^2 \qquad (1)$$

where the integration is over the electron coordinates, x. H is the electronic Hamiltonian, R is the internuclear distance, φ_ε is the orbital of the "free" electron with energy ε and Φ_{ion} and Φ_d are the multiconfiguration wave functions of the ion and dissociative states. The widths are calculated as described previously [5] by substituting a high principal quantum number Rydberg orbital for the "free electron" and multiplying the matrix element in (1) by a density of states. An R dependent width of the form of (1) needs to be calculated for each of the ion states. The width connecting the dissociative state to the A core states is needed to describe the predissociation of ECR states. In terms of real orbitals, the dominant configurations in the b′ state at R=2.0 a_o are

$$\ldots 3\sigma_g^2\ 1\pi_{ux}^2\ 1\pi_{uy}\ \ 1\pi_{gy} + \ldots 3\sigma_g^2\ 1\pi_{ux}\ 1\pi_{uy}^2\ 1\pi_{gx} \qquad (2)$$

where … denotes the inner orbitals, $1\sigma_g^2\ 1\sigma_u^2\ 2\sigma_g^2\ 2\sigma_u^2$. The dominant configurations of the ion states plus a "free" electron, φ_ε , in $^1\Sigma_u^+$ symmetry are

$$\ldots 3\sigma_g\ 1\pi_{ux}^2\ 1\pi_{uy}^2\ \varphi_\varepsilon(\sigma_u) \qquad (3)$$

for $X^2\Sigma_g^+$ and

$$\ldots 3\sigma_g^2\ 1\pi_{ux}\ 1\pi_{uy}^2\ \varphi_\varepsilon(\pi_{gx})\ +\ \ldots 3\sigma_g^2\ 1\pi_{ux}^2\ 1\pi_{uy}\ \varphi_\varepsilon(\pi_{gy}) \qquad (4)$$

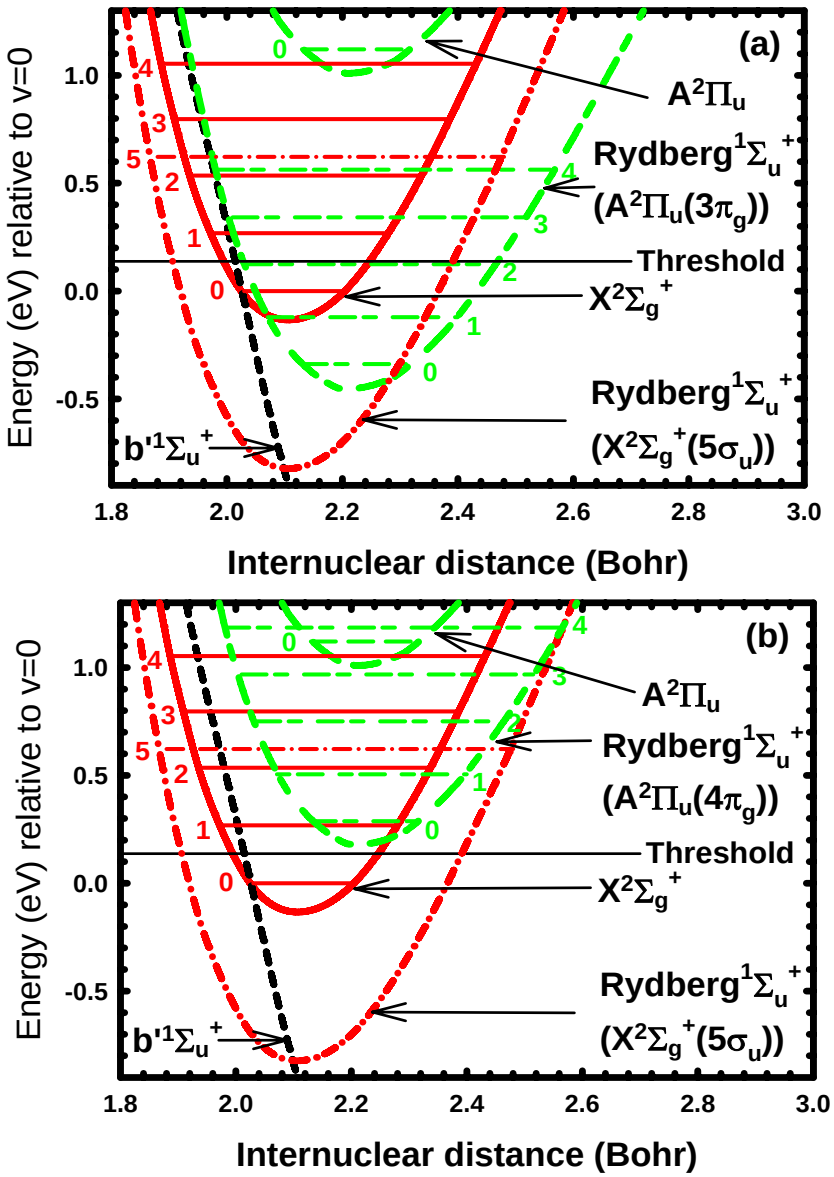

Figure 1. (a) Potential curves are shown for the ground state of the ion (solid, red online), the n=5 ground core Rydberg state (dot-dash, red online), the A state of the ion (long dash, green online) and the dissociative $b'^1\Sigma_u^+$ (short dash, black online). Numbered vibrational levels for the ion and Rydberg states are also shown. The large R asymptote of the b′ state is shown by the horizontal line labeled "threshold." Also shown is the potential curve for $^1\Sigma_u^+$ (($A^2\Pi_u$) $3\pi_g$) (long short dash, green online). (b) Same as (a) except that the $^1\Sigma_u^+$ (($A^2\Pi_u$) $4\pi_g$) (long short dash, green online) potential curve is shown in place of the $3\pi_g$ state.

for $A^2\Pi_u$. Since the dissociative state has $^1\Sigma_u^+$ symmetry and the Hamiltonian in equation (1) transforms as $^1\Sigma_g^+$, a nonzero width results only if the ion plus a free electron (or a Rydberg state) wave

function also has $^1\Sigma_u^+$ symmetry and thus the σ_u "free orbital" is coupled to the X state and the $1\pi_g$ "free orbital" is coupled to the A state.

The dissociative state differs from the X state plus a continuum electron by a double excitation, i.e. two electrons must be moved from the orbitals in (2) to obtain the configuration in (3). However, only a single excitation ($\varphi_\varepsilon(\pi_g) \rightarrow (1\pi_g)$) is required to change the configurations in (2) to that for (4). Valence and electron-ion states that differ by a single excitation are connected by large widths. This is borne out by our calculations which show that the electronic width for the A core state plus a continuum electron is 4.0 eV near R=2.1 a_o. The width for the X core state plus a continuum electron is 0.36 eV near R=2.1 a_o.

An additional width used in the cross section calculations is that connecting the X and A core continuum states, i.e.,

$$\Gamma(R, \varepsilon, \varepsilon') = 2\pi <\{\Phi_X(x, R)\, \varphi_\varepsilon(x, R)\} \,|H|\, \{\Phi_A(x, R)\;\; \varphi'_{\varepsilon'}(x, R)\} >^2. \qquad (5)$$

However, using a similar approach to that described previously [5], the calculated value of the width in (5) is zero to two decimal places at R=2.3 a_o. Therefore, a width of zero at all internuclear distances has been used in the cross section calculation. The excited core states can still mix with the ground core states by a second order interaction in which the dissociative state acts as an intermediate. In this mechanism, the dissociative state, which predissociates the Rydberg states of both cores, in turn allows the Rydberg states to mix and allows the ECR levels to autoionize to the ground core continuum. This interaction is included in the Multichannel Quantum Defect Theory (MQDT) approach described below for calculating the cross sections and rate constants. The second order K matrix element is given by [18]:

$$K_{vv'}^{E_T} = \mathbf{P}\int dE(\langle\chi_v|V|F_d(E)\rangle\langle F_d(E)|V|\chi_{v'}\rangle/(E_T-(E_d+E)) \qquad (6)$$

where v and v′ run over the bound vibrational levels of the X and A core ion states or of the Rydberg levels. **P** is the principal value operator, the χ_v are the bound vibrational wave functions, F_d is the continuum vibrational wave function of the dissociative state, V is the electronic part of the matrix element given in equation (1), E_T is the total energy, E_d is the energy of the asymptote of the dissociative curve, E is the kinetic energy of the dissociating atoms so that $E_T = E_d + E$. The matrix element in equation (6) describes the mixing of vibrational levels among a single state of the ion or the mixing of levels between the X and A states. The mixing is due to the dissociative state. Further comment on equation (6) is given below.

As described previously [5], the quantum defect is determined from the energy difference, ΔE, between the Rydberg state used in the width matrix elements and the ion. The quantum defect is defined by $\mu(R) = n - 1/(2\Delta E(R))^{1/2}$ where n is the principal quantum number and ΔE is the binding energy of the Rydberg orbital. Quantum defects for the $^1\Sigma_u^+$ Rydberg series converging to the X and A ion states are both included in the calculations.

4. Cross Sections

The DR cross sections have been calculated with the MQDT approach [16-18] using the second order of the K matrix [18]. The calculations include 18 vibrational levels in the ground ion potential, 18 in the A state potential and 18 in each of the Rydberg states for both the ground and excited cores. All vibrational wave functions were calculated on a 0.001 a_o grid from an internuclear distance of 1.0 to 8.0 a_o. Cross sections were calculated on an energy grid of 0.0001 eV from threshold to 1.0 eV.

If only the ground state ion core is included in the calculation, the cross section appears as shown in figure 2a. Note that the cross section starts at an electron energy of 0.137 eV corresponding to the position of the dissociative state asymptote. The direct cross section (dashed, green on line) has steep drops as new autoionization channels open at 0.27 eV (v=1), 0.54 eV (v=2) and 0.80 eV (v=3). The

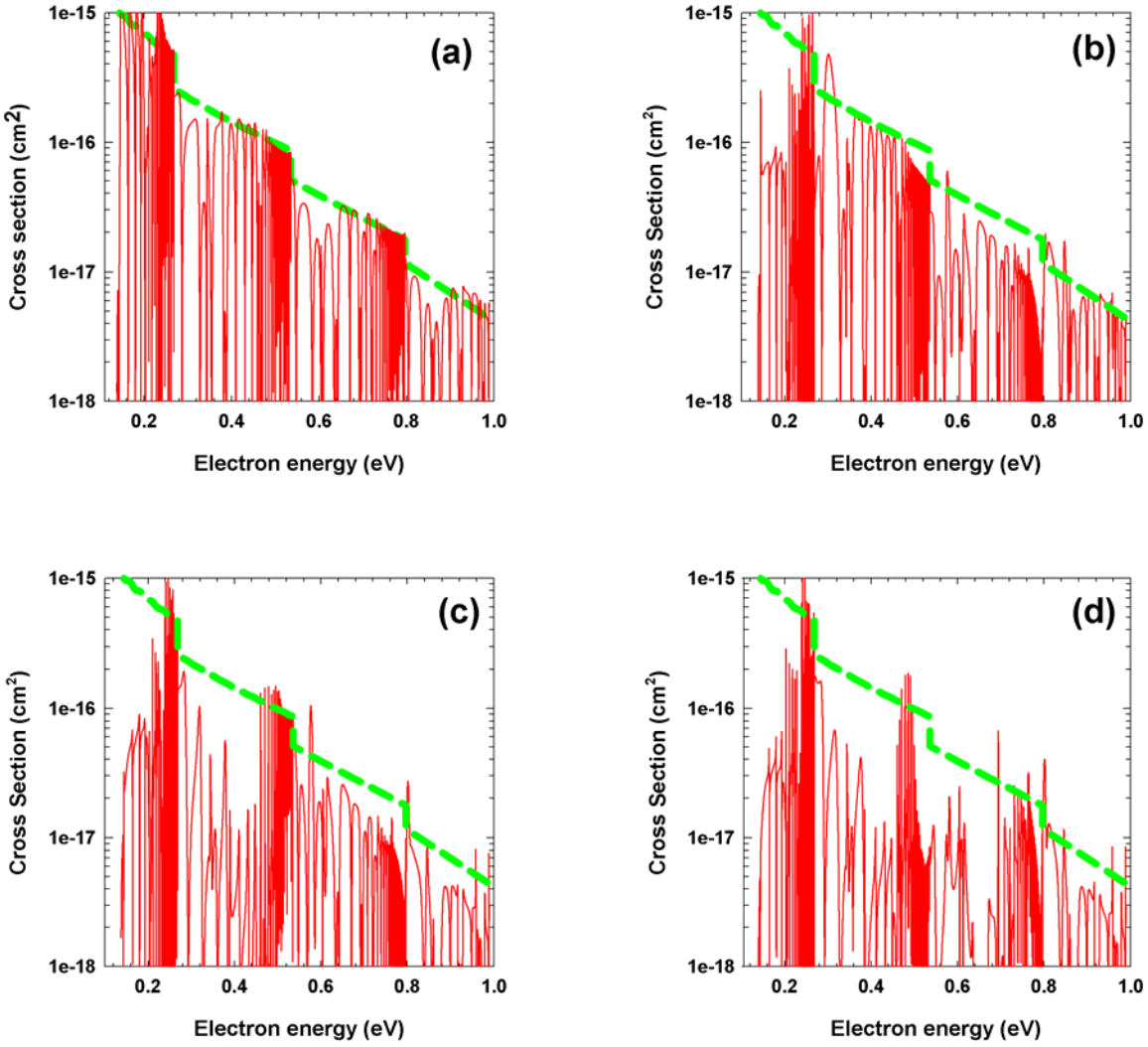

Figure 2. DR cross section for the $^1\Sigma_u^+$ dissociative route. (a) Only the ground ion core states are included. The direct cross section is the dashed line (green online) and the full cross section is the solid line (red online). (b), (c) and (d) are the same as (a) except that the v=0-2, v=0-3 and v=0-4 levels respectively of the A core Rydberg states are included.

full cross section (solid line, red online) includes structure due to the Rydberg resonances.

Below the energy of each ion vibrational threshold there is a pile up of Rydberg states having that level as the series limit. The resonances appear mostly as dips falling below the direct cross section. This is a characteristic cross section for a dissociative curve that crosses the ion within or near the turning points of v=0.

The large width for the A core states indicates that an MQDT treatment that includes K matrix terms beyond second order may be needed. However, it is important to note that the vibrational overlaps for the excited core are low and the factor of about 10 by which the excited core electronic width exceeds the ground core width is much larger than the factor separating the K matrix elements. The largest K matrix elements (unitless) are about 2.0 and correspond to mixing among excited core vibrational levels due to the dissociative state (see previous section). The largest K matrix element

among ground core levels is 0.6 and corresponds to the direct interaction of the v=1 level with the dissociative state. Nevertheless, a calculation using a K matrix beyond second order would be worthwhile.

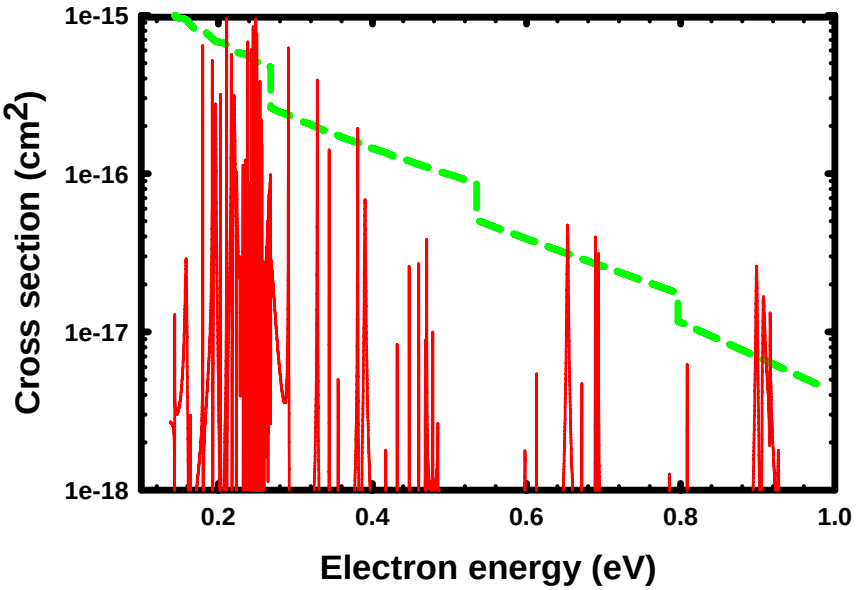

Figure 3. Same as figure 2a except that 18 Rydberg vibrational levels for both the ground core and the A state are now included.

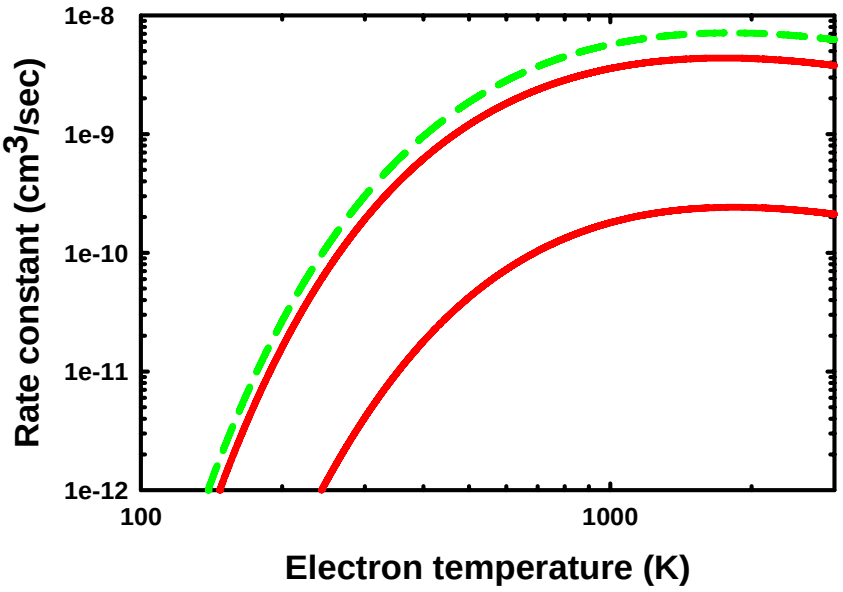

Figure 4. Rate constants for DR. The dashed curve is the direct rate constant. The upper and lower solid curves include X core resonances and X + A core resonances respectively.

In order to understand the important role of the excited core states, we explore the change induced in the total cross section due to the addition of individual ECR vibrational levels. From figure 1b it can be seen that the first v=0 Rydberg level with the A core lies at about 0.3 eV above the v=0 level of the ground ion and has n=4. However, figure 1b shows that the v=0 ECR level has little overlap with the dissociative vibrational wave function. For v=1, the first ECR level occurs at about 0.5 eV electron energy (see figure 1b). As for v=0, the low overlap of the v=1 resonances with the dissociative vibrational wave function relegates these resonances to a negligible role. The situation is however different for the ECR n=3, v=2 resonances. Figure 1a shows that this resonance is found at an electron energy near 0.137 eV, i.e. near the threshold for DR. Because the vibrational overlap with the dissociative vibrational wave function is higher than that with v=0, 1, this resonance will notably affect DR at the threshold. Figure 2b shows the cross section including 18 vibrational levels for ground ion states and the lowest three vibrational levels of the ECR states. A pronounced drop is seen in the cross section just above threshold due to the n=3, v=2 A core state. The v=2 A core states have a large K matrix element (0.28) with the v=0 ground core continuum and with the v=1 ground core levels (-0.38). These matrix elements are all of the form of the second order term given in equation (6) and involve the dissociative state acting as an intermediate. The net effect of these interactions is to lead to an increase in autoionization and a large drop in the DR cross section just above threshold.

From figure 1b, the next v=2 state occurs for n=4 at about 0.75 eV, just below the v=3 level of the ground core ion. The ground core v=3 levels have a large K matrix element with excited core v=2 levels (0.39). With the large K matrix element connecting the v=2 ECR states with the ground core continuum, the result is the destructive interference shown in figure 2b at 0.75 eV. Note that the cross section drop near 0.52 eV is due to the second order interaction (-0.38) of the A core, n=4, v=1 level with the ground core v=2 levels. The cross section drops because the A core v=1 levels have a large second order interaction (-0.45) with the v=0 ground core continuum leading to an increase in the probability for autoionization.

Addition of the v=3 ECR resonances leads to the cross section shown in figure 2c. The lowest resonance, n=3 (see figure 1a), is near 0.34 eV. Comparing figures 2b and 2c, the n=3 resonance annihilates the cross section structure near 0.34 eV by nearly an order of magnitude. The next v=3 resonance, n=4, falls at about 0.96 eV (see figure 1b), and also affects the structure in this region.

Figure 2d shows the resulting cross section that includes the v=0-4 ECR resonances. Once again, a large degree of destructive interference occurs near 0.56-0.66 eV due to the n=3, v=4 ECR resonance which has a large K matrix element (-0.57) with the v=3 ground core states. The final cross section including 18 vibrational levels in the A core states is in figure 3. The A core Rydberg states have annihilated most of the cross section due to the ground core states.

The rate constants for the two cases are shown in figure 4. As might be expected, the rate constant for the case in which the excited ion core is included is much smaller than that which results from only the ground core states. Because of the threshold of 0.137 eV for DR from v=0, the rate constant at room temperature is very small, 4.1 x 10^{-12} cm^3/sec. At 1000K electron temperature, the full rate constant is 1.8 x 10^{-10} cm^3/sec compared to 3.6 x 10^{-9} cm^3/sec if only ground core resonances are included.

5. Conclusions

DR along the $b'^1\Sigma_u^+$ dissociative state from the v=0 ion vibrational level has a low rate constant at room temperature because DR can only occur for electron energies above 0.137 eV. The addition of the A core Rydberg states decreases the rate coefficient by a factor of 20 at 1000 K electron temperature. The decrease is due to the large electronic width of the excited core states which increases the probability of autoionization. The autoionization probability is high because the ECR levels are connected to the ionization continuum of the v=0 ground ion by large second order K matrix terms. In these terms the dissociative state provides the coupling between the ECR levels and the ground ion continuum. It is clear that ECR states cannot be neglected in this case if an accurate

description of DR is desired. A further study of the role of the ECR states in this case with a higher order K matrix is planned.

Acknowledgements
This material is based upon work supported by the National Science Foundation under Grant No. ATM-0225256. Any opinions, findings, and conclusions or recommendations expressed in this material are those of the author and do not necessarily reflect the views of the National Science Foundation. This research is also supported by NASA grants NNG05GO93G and NNG05GI34G.

References
[1] Bates D R 1950 *Phys. Rev.* **78** 492
[2] Bardsley J N 1968 *J. Phys. B* **1** 365
[3] Guberman S L Ab initio studies of Dissociative Recombination, in *Dissociative Recombination: Theory, Experiment and Applications*; Mitchell, J. B. A., Guberman, S. L. Eds.; World Scientific: Singapore, 1989; p 45
[4] Guberman S L New Mechanisms for Dissociative Recombination, in *The Physics of Electronic and Atomic Collisions, Invited Papers for the XIX International Conference*; Dube, L. J., Mitchell, J. B. A., McConkey, J. W., Brion, C. E., Eds.; American Institute of Physics Press: New York, 1995; p 307
[5] Guberman S L 2007 *J. Phys. Chem. A* **111** 11254
[6] Forck P et al. 1994 *Phys. Rev. Lett.* **72** 2002
[7] Amitay Z et al. 1996 *Phys. Rev. A* **54** 4032
[8] Carata L, Orel A E, Schneider I F and Suzor-Weiner A Core Excited Resonances in the Dissociative Recombination of CH^+ and CD^+, in *Dissociative Recombination: Theory, Experiment and Applications*; Larssen M, Mitchell J B A and Schneider I F, Eds.; World Scientific: Singapore, 2000; p 291.
[9] Carata L, Orel A. E., Raoult M., Schneider I F, Suzor-Weiner A 2000 Phys. Rev. A **62** 052711
[10] Amitay Z et al. 1996 *Phys. Rev. A* **53** R644
[11] Guberman S L 1983 *J. Chem. Phys.* **78** 1404
[12] Guberman S L 1991 *Geophys. Res. Lett.* **18** 1051
[13] Dunning, Jr. T H 1989 *J. Chem. Phys.* **90** 1007
[14] Lofthus A and Krupenie P H 1977 *J. Phys. Chem. Ref. Data* **6** 113
[15] Moore, C E Atomic Energy Levels, Vol. I (US Dept. of Commerce, Washington, DC, 1971)
[16] Giusti, A 1980 *J. Phys. B* **13** 3867
[17] Lee, C M 1977 *Phys. Rev. A* **16** 109
[18] Guberman S L and Giusti-Suzor A 1991 *J. Chem. Phys.* **95** 2602